Ternary fission of superheavy elements

M. Balasubramaniam* and K. R. Vijayaraghavan
Department of Physics, Bharathiar University, Coimbatore 641046, India.

K. Manimaran
Department of Physics, Government Arts College, Udumalpet 642126, India

(Received 9 October 2015; revised manuscript received 4 November 2015; published 4 January 2016)

Ternary fission of superheavy nuclei is studied within the three-cluster model potential energy surfaces (PESs). Due to shell effects, the stability of superheavy nuclei has been predicted to be associated with $Z = 114$, 120, and 126 for protons and $N = 184$ for neutrons. Taking some representative nuclei we have extended the ternary fission studies to superheavy nuclei. We adopted two minimization procedures to minimize the potential and considered different arrangements of the fragments. The PES from one-dimensional minimization reveals a strong cluster region favoring various ternary breakups for an arrangement in which the lightest fragment is kept at the center. The PES obtained from two-dimensional minimization reveals strong preference of ternary fragmentation in the true ternary fission region. Though the dominant decay mode of superheavy nuclei is α decay, the α-accompanied ternary breakup is found to be a nonfavorable one. Further, the prominent ternary combinations are found to be associated with the neutron magic number.

DOI: 10.1103/PhysRevC.93.014601

I. INTRODUCTION

Flerov [1] suggested the use of a highly neutron-rich beam of $^{48}_{20}$Ca on actinide targets such as $^{244}_{94}$Pu, $^{248}_{96}$Cm and $^{252}_{98}$Cf for the synthesis of superheavy nucleus (SHN); he succeeded in synthesizing $^{252}_{102}$No in a cold reaction with $^{206}_{82}$Pb targets [2]. Fiset and Nix predicted [3] that the nucleus with $Z = 110$ and $N = 184$ has a longer total half life of $T_{1/2} = 10^9$ years. In the discussion section of Ref. [4], Nix, suggested the use of very asymmetric target projectile combinations, such as $^{250}_{96}$Cm and $^{257}_{100}$Fm with $^{48}_{20}$Ca to synthesize superheavy nuclei. Gupta *et al.* also suggested [5] that the use of a ^{48}Ca beam on even-even $^{196-204}$Hg, $^{204-208}$Pb, ^{232}Th, $^{234-238}$U, $^{240-244}$Pu, and $^{244-248}$Cm targets for synthesizing various isotopes of even $Z = 100$, 102, and 110–116 elements. The synthesis of a superheavy nucleus has natural limitations due to the decrease in half lives with increase in charge number. The stabilization of SHN is mainly attributed to the shell effects [6–8] since the SHN possess an almost negligible liquid drop fission barrier. Based on the liquid drop picture it had been envisioned that a nucleus can split into two, three, or more and the energy release would be larger if the division is more than two. In the heavy element region, splitting into two, the so-called binary fission, is the predominant breakup with less probability of breakup into three or more fragments. Since the fission barrier picture has ruled out the possibility of the binary breakup of a superheavy nucleus leading to fission, the other possible fission modes are not investigated rigorously in this region.

α emission is the dominant decay mode in the superheavy region, i.e., the superheavy nucleus predominantly undergoes sequential α decays followed by spontaneous fission. Binary fission being not a feasible decay mode, cluster decay is predicted as a possible decay mode in the superheavy region. Kumar *et al.* predicted [9] that in addition to α decay and fission, emission of heavy clusters, such as ^{14}C, ^{34}Si, and/or Ca, are possible cases of cluster decay modes for any of the parent superheavy nuclei of the $^{277}_{110}$X α-decay chain.

Based on liquid drop model prediction, several theoretical and experimental studies were made to explore the ternary fission in transactinide region. But very few experiments [10–12] were carried out to observe ternary fission in the superheavy system formed in heavy-ion reactions. Fleischer *et al.* measured [10] the ternary to binary ratio from the superheavy system formed in the interaction of Th and 414 MeV Ar ions. Becker *et al.* measured [11] the ternary to binary ratio of the superheavy system formed while uranium is irradiated with 540 MeV Fe ions. They observed the symmetric ternary fission events with the aid of a microscope and detected tracks of the fragments through mica detectors. Vater *et al.* investigated [12] experimentally the symmetric ternary fission for the system formed in the reaction of U+Ar. Wild *et al.* measured [13] the energy distribution and the emission probabilities of light charge particles (^{1}H, ^{3}H, and ^{4}He) from the spontaneous fission of superheavy nuclei ^{256,257}Fm. Apart from this Grumann *et al.* reported [14] that superheavy nuclei undergo ternary fission through oblate deformation and predicted ternary fission as the dominant decay mode of superheavy nuclei. Later Diehl and Greiner [15,16] have shown that in $^{298}_{114}$X the liquid drop barrier for oblate ternary fission is more than 50 MeV high and suggested that oblate ternary fission can be ruled out since the shell energy of nearly magic nuclei can hardly reduce this barrier. Contrary to that, the prolate liquid drop barriers almost vanish and they have equal heights for binary and ternary fission of the superheavy nuclei with mass number of about 300 [16].

*m.balou@gmail.com

Schultheis *et al.* calculated [17] the barrier for ternary fission of superheavy nuclei and reported that unlike actinides the barriers for binary and ternary fission are equal within 10%. They also calculated the relative cross section (σ_T/σ_B) of ternary to binary spontaneous fissions, which is much higher in the superheavy nuclei than in the actinide region. They justified this result by the following reason; in binary fission of superheavy nuclei many nucleons would be outside the closed shell ($Z = 50$, $N = 82$) of both the fragments, hence it might be energetically favorable to form a third cluster (with neutron or proton magic number of nucleons) among these nucleons (say, for example, $^{132}\mathrm{Sn} + ^{132}\mathrm{Sn} + ^{34}\mathrm{Si}$ in $^{298}_{114}\mathrm{X}$). For actinides, a lower number of nucleons are available outside the closed shells. With this successful justification they extended [18] their calculation to 20 even mass nuclei in the region of $110 \leqslant Z \leqslant 122$ and $176 \leqslant N \leqslant 192$. From their calculations it is reported that ternary fission barriers in this superheavy mass region exceed the binary barriers by only 10–35 %. Minimum excess of the ternary barrier height over the binary one occurs in the region below the doubly magic nucleus $^{298}_{114}\mathrm{X}$, where the total life time is high with respect to spontaneous fission and α and β decay. This result implies that the ratio of ternary to binary will be large for highly stable superheavy nuclei. Hence, the high ternary to binary ratio is considered as a characteristic property of superheavy nuclei and it is advocated as a test for superheavy elements. If the measured relative counting rate Γ_T/Γ_B is substantially larger than 10^{-6} then the event has to be associated with superheavy nuclei. Schultheis *et al.* calculated [19] the ternary and binary fission barriers and their relative penetrability for the isotopes $184 \leqslant N \leqslant 228$ of element $Z = 126$, considering both $Z = 114$ and 126 as magic numbers in the calculation of shell energy. In all the cases the predicted ternary to binary relative rates Γ_T/Γ_B are substantially higher than those for actinides.

Greiner predicted that ternary fission could be a possible decay mode for superheavy nuclei though fission remains a noncompeting decay mode, with respect to α decay. To our knowledge, since then there has been no other significant progress in the theoretical (or experimental) study of ternary fission in superheavy mass region. Very recently Zagrebaev *et al.* studied [20] the possibility of true ternary fission in superheavy nuclei and reported that it is quite possible for superheavy nuclei to undergo ternary fission, with formation of a heavy third fragment because of the strong shell effects leading to a three-body clusterization with the two doubly magic Sn-like cores (for example $^{132}\mathrm{Sn} + ^{132}\mathrm{Sn} + ^{32}\mathrm{S}$ in $^{296}_{116}\mathrm{X}$). All these theoretical predictions [14,17–19] and experimental observations [10–12,20] imply that ternary fission might be a competing decay mode to α decay in the superheavy mass region. Hence, it would be of interest to see the possibilities of observing heavy light charged particles with doubly magic Sn-like main fission fragments in spontaneous ternary fission of highly stable superheavy nuclei. On the structure side, the relativistic mean-field theory [21] predicted the next magic number for SHN as $Z = 120$ and $N = 172$ or 184. The nonrelativistic model [22–25] shows that there will be closed shells at $Z = 114$ and $N = 184$. Cwiok [26] *et al.* predicted the next proton magic number as $Z = 126$. Based on these facts, for this study we have chosen three nuclei with $Z = 114$, 120, and 126 and the neutron number as 184 for all the three nuclei *viz.*, $^{298}_{114}\mathrm{X}$, $^{304}_{120}\mathrm{X}$, and $^{310}_{126}\mathrm{X}$.

II. METHODOLOGY

Within the three-cluster model (TCM) [27–32], the ternary fragmentation potential between the three (spherical) fragments in collinear geometry is the sum of the total Coulomb potential, the total nuclear potential, and the sum of the mass excesses of the ternary fragments and it can be written as

$$V_{\mathrm{tot}} = \sum_{i=1}^{3} m_x^i + \sum_{i=1}^{3}\sum_{j>i}^{3} V_{Cij} + V_{Pij}, \tag{1}$$

where m_x^i are the mass excesses of the three fragments in energy units, taken from Ref. [33].

The Coulomb interaction energy V_{Cij} defines the force of repulsion between two of the interacting charges. The Coulomb expression is defined as,

$$V_{C_{ij}} = \frac{Z_i Z_j e^2}{R_{ij}}, \tag{2}$$

where R_x is the radius of the fragment, it is defined by $R_x = 1.28A_x^{1/3} - 0.76 + 0.8A_x^{-1/3}$ fm. (x is taking the values of 1, 2, and 3 corresponding to fragments A_1, A_2, and A_3). R_{ij} is the center to center distance between the fragments i and j.

The proximity potential V_{Pij} is defined as

$$V_{Pij} = 4\pi\overline{R}\gamma b\phi(\xi). \tag{3}$$

The universal function $\phi(\xi)$ depends only on the distance between two nuclei and is independent of the atomic numbers of the two nuclei, it is given by

$$\phi(\xi) = \begin{cases} -\frac{1}{2}(\xi - 2.54)^2 - q(\xi - 2.54)^3, & \xi < t \\ -3.437\exp(-\xi/0.75), & \xi \geqslant t. \end{cases} \tag{4}$$

Here, $q = 0.0852$, $t = 1.2511$, and $\xi = s/b$, which takes negative (the overlap region), zero (for touching configuration), and positive (separated configurations) values of s ($= R_{ij} - R_i - R_j$). b is the diffusivity parameter of the nuclear surface given by $b = 0.99$ fm. The specific nuclear surface tension γ is given by

$$\gamma = 0.9517\left[1 - 1.7826\left(\frac{N-Z}{A}\right)^2\right]\mathrm{MeV\ fm^{-2}}. \tag{5}$$

The mean curvature radius, $\overline{R}$ has the form

$$\overline{R} = \frac{R_i R_j}{R_i + R_j}. \tag{6}$$

In TCM the available Q value to the kinetic energies E_i of the three fragments, i.e., $Q = E_1 + E_2 + E_3$, is defined as

$$Q = M - \sum_{i=1}^{3} m_x^i, \tag{7}$$

where M and m_x^i are the mass excess of the decaying nucleus and the product nuclei respectively, which are expressed in MeV and taken from Ref. [33].

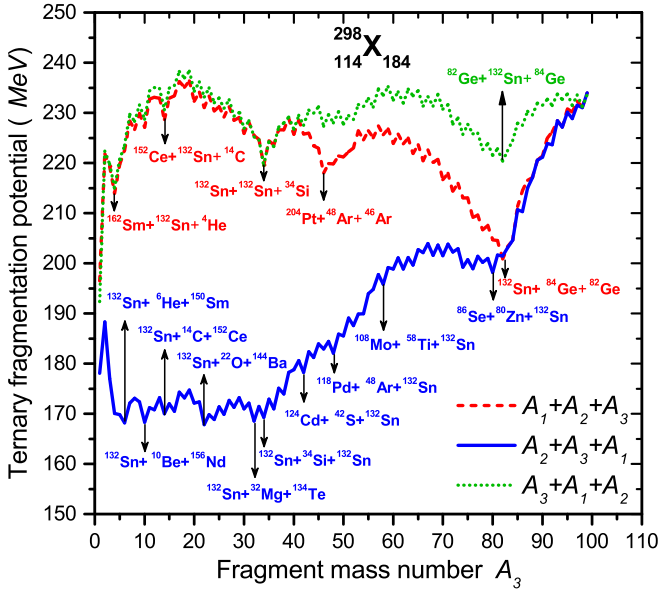

FIG. 1. Ternary fragmentation potential of $^{298}_{114}$X as a function of fragment mass number A_2 for three different arrangements.

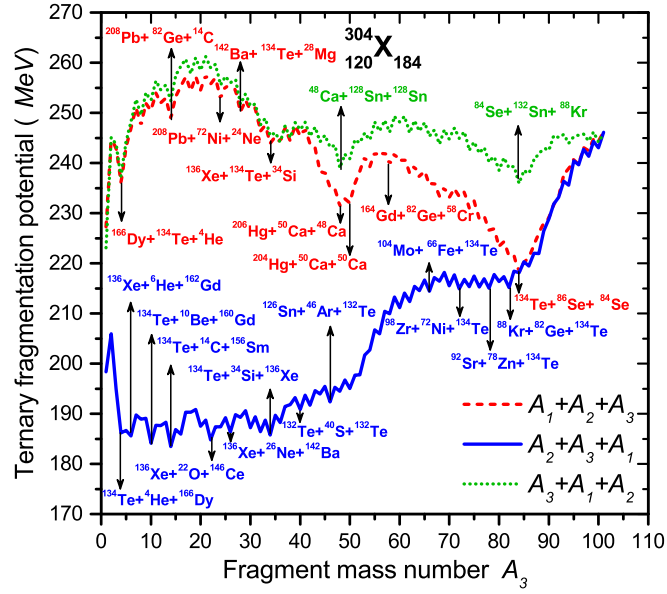

FIG. 2. Same as Fig. 1, but for $^{304}_{120}$X.

III. RESULTS AND DISCUSSIONS

The potential energy surfaces (PESs) for the superheavy nuclei considered are calculated by imposing the condition $A_1 \geqslant A_2 \geqslant A_3$ on the masses such that the fragment combinations are not repeated. A_1, A_2, and A_3 are the mass numbers of the three fragments. A_1 is considered as the heaviest among all the three fragments and A_3 as the lightest among all the fragments. All the three fragments may have the same mass also. The minimization of the potential was done as discussed in Ref. [34].

Thus obtained minimized potentials are plotted with respect to the third fragment mass number A_3 as shown in Figs. 1, 2, and 3 for the ternary fission of $^{298}_{114}$X, $^{304}_{120}$X, and $^{310}_{126}$X, respectively. In each figure, the three different potential energy curves correspond to three different arrangements *viz.*,

(i) Case I: keeping A_2 in the middle;
(ii) Case II: keeping A_3 in the middle; and
(iii) Case III: keeping A_1 in the middle.

It is to be mentioned here that these three cases correspond to collinear configuration. Recently, we have shown in Ref. [36] that collinear configuration as a favorable configuration over triangular configuration particularly for heavy third fragments. Further, the potential energy is always higher for Case III, which indicates that the formation of heaviest fragment at the middle is not a favorable configuration, and can be ruled out for further analysis as is also shown in Ref. [36]. In the present discussion we limit only to Cases I and II and a representative result of triangular configuration.

It can be seen from the Figs. 1, 2, and 3 that the structure of the potential corresponding to Case II (solid line) is altogether different from Cases I and III. For lower mass numbers, say $A_3 < 40$, and for almost equal mass numbers beyond $A_3 > 80$, the potential energies corresponding to Case I and Case III are more or less similar. Case II is of our interest in which a region of mass numbers from 1–40 shows some significant results. In this region, several light mass nuclei (clusters) are having very low potential energy compared to Cases I and III. This result implies that during the ternary breakup, the formation of a light mass nucleus (A_3) at the middle is having higher probability. For mass numbers $A_3 > 40$, the potential energy increases linearly. Comparing the Figs. 1, 2, and 3, it is seen that the cluster region broadens with increase in mass number of parent nuclei.

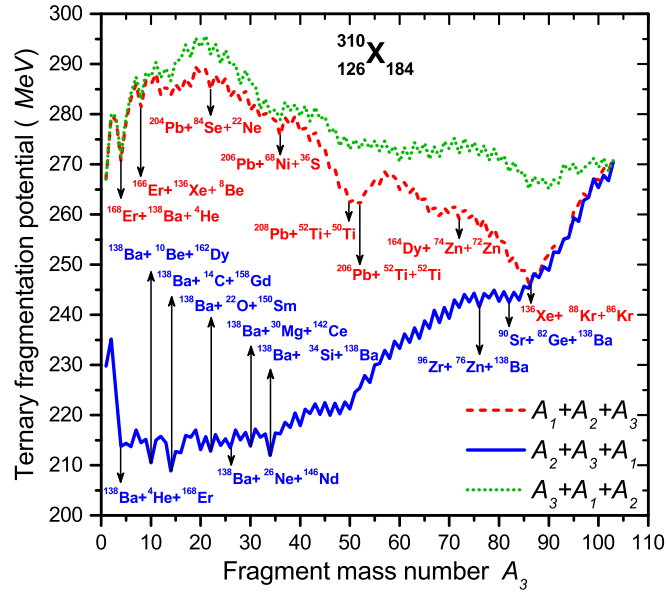

FIG. 3. Same as Fig. 1, but for the parent nucleus $^{310}_{126}$X.

For the true ternary breakup of $^{298}_{114}$X, with comparable masses, corresponding to Case II, the fragment combination $^{86}_{34}$Se + $^{80}_{30}$Zn + $^{132}_{50}$Sn seems to be a probable one as shown in Fig. 1. In addition, there are other pronounced valleys for the fragment combinations $^{132}_{50}$Sn + $^{22}_{8}$O + $^{144}_{56}$Ba, $^{132}_{50}$Sn + $^{32}_{12}$Mg + $^{134}_{52}$Te, and $^{132}_{50}$Sn + $^{34}_{14}$Si + $^{132}_{50}$Sn (as marked in Fig. 1) in the potential energy. These combinations are having two fragments with closed shell. For the Case I (dashed line), there are several combinations possessing a deep minimum in PES. For these combinations, the neutron number of the fragments is associated with a magic number particularly for the fragments in the combinations $^{132}_{50}$Sn + $^{132}_{50}$Sn + $^{34}_{14}$Si and $^{204}_{78}$Pt + $^{48}_{18}$Ar + $^{46}_{18}$Ar of $^{298}_{114}$X, $^{208}_{82}$Pb + $^{82}_{32}$Ge + $^{14}_{6}$C, and $^{206}_{80}$Hg + $^{50}_{20}$Ca + $^{48}_{20}$Ca of $^{304}_{120}$X and the combinations $^{208}_{82}$Pb + $^{86}_{36}$Kr + $^{16}_{8}$O and $^{136}_{54}$Xe + $^{88}_{36}$Kr + $^{86}_{36}$Kr of $^{310}_{126}$X are having minimum potential energies.

From the ternary fragmentation potential energy surface of $^{304}_{120}$X corresponding to the Case II arrangement, as shown in Fig. 2, it is seen that the fragment combinations $^{98}_{40}$Zr + $^{72}_{28}$Ni + $^{134}_{52}$Te, $^{92}_{38}$Sr + $^{78}_{30}$Zn + $^{134}_{52}$Te, and $^{88}_{36}$Kr + $^{82}_{32}$Ge + $^{134}_{52}$Te are having minimum potential energy in the true ternary fission region. In addition to that there are several combinations having notable minimum potential energy in the cluster region viz., $^{134}_{52}$Te + $^{10}_{4}$Be + $^{160}_{64}$Gd, $^{134}_{52}$Te + $^{14}_{6}$C + $^{156}_{62}$Sm, $^{136}_{54}$Xe + $^{22}_{8}$O + $^{146}_{58}$Ce, and $^{134}_{52}$Te + $^{34}_{14}$Si + $^{136}_{54}$Xe. In Fig. 3 for the Case II arrangement, it is seen that the fragment combinations $^{96}_{40}$Zr + $^{76}_{30}$Zn + $^{138}_{56}$Ba and $^{90}_{38}$Sr + $^{82}_{32}$Ge + $^{138}_{56}$Ba are having minimum potential energy in the true ternary fission region. Further, there are several combinations having minimum potential energy in the cluster region, namely $^{138}_{56}$Ba + $^{10}_{4}$Be + $^{162}_{66}$Dy, $^{138}_{56}$Ba + $^{14}_{6}$C + $^{158}_{64}$Gd, and $^{138}_{56}$Ba + $^{22}_{8}$O + $^{150}_{62}$Sm. From Figs. 1, 2, and 3, it is seen that the fragments with the neutron magic number dominate over the fragments with the proton magic number and at least one of the fragments in the combination is either proton or neutron closure.

Further, the calculated Q value is found to be higher for the fragment combinations having heavier third fragments, indicating a strong preference to the true ternary fission. From these figures, it can be seen that the ternary breakup with the lightest fragment at the middle has more probability than the other two arrangements. The strong decrease in the potential for Case II is due to the fact that the Coulomb potential between the fragments A_1 and A_2 reduces considerably as they are separated at least by the diameter of the lightest fragment A_3.

Two-dimensional minimization

In the foregoing discussion all possible combinations are minimized with respect to the mass number of the third fragment A_3. All possible combinations are classified into a number of groups according to the mass number of the third fragment, i.e., the ternary combinations having the same mass number A_3 are combined to form one group. The third fragment mass number will vary from 1 to integer number of $\frac{A}{3}$, where A is the mass number of the parent nucleus. In each group thus formed, we search for a combination having minimum potential energy among all the combinations. In this way, we get the $\frac{A}{3}$ minimized combinations that are the most favorable combinations. This minimization can be done separately for the different arrangements of the fragments, referred to as Cases I, II, and III.

In order to get an overall picture about all possible minimized combinations, we follow a two-dimensional minimization procedure in which all the possible combinations are minimized with respect to the charge and/or neutron number of the three fragments. For this minimization, a two-dimensional array is defined to choose the best combinations from all possible combinations. All possible combinations are classified into a number of groups according to the charge number of the fission fragments in the combinations, i.e., the ternary combinations having the same charge numbers Z_1, Z_2, and Z_3 are combined to form one group. The number of

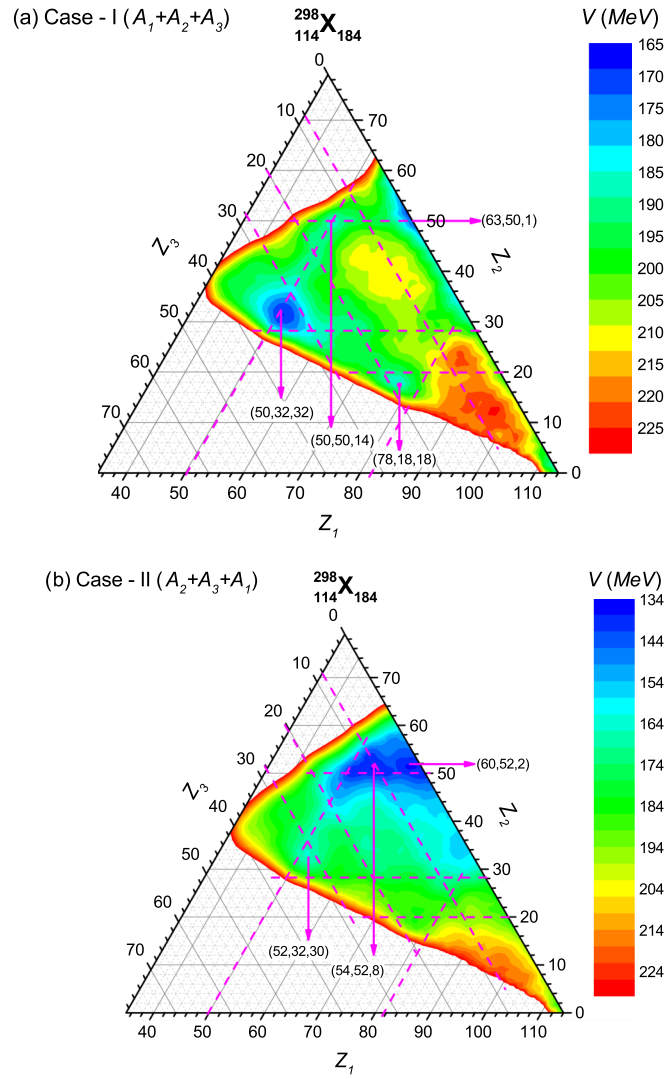

FIG. 4. Potential energy surfaces of proton-minimized ternary fission fragments at touching configuration for the arrangements (a) Case I (upper) and (b) Case II (lower) in the ternary fission of $^{298}_{114}$X.

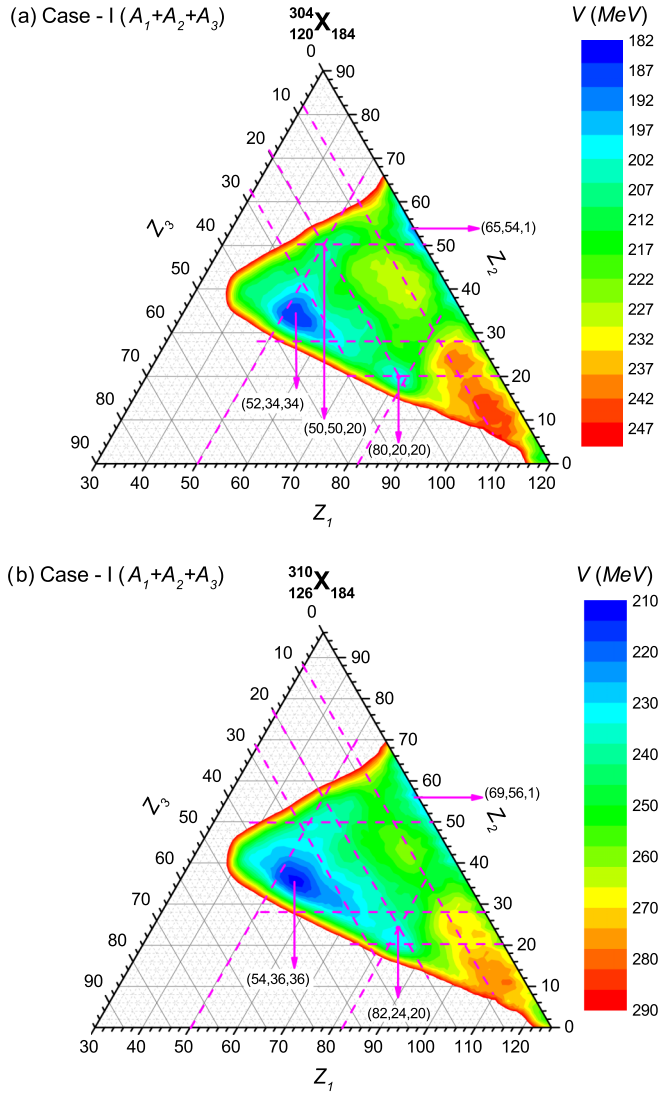

FIG. 5. Potential energy surfaces of proton-minimized ternary fission fragments at touching configuration for the arrangement Case I in the fission of (a) $^{304}_{120}$X (upper) and (b) $^{310}_{126}$X (lower).

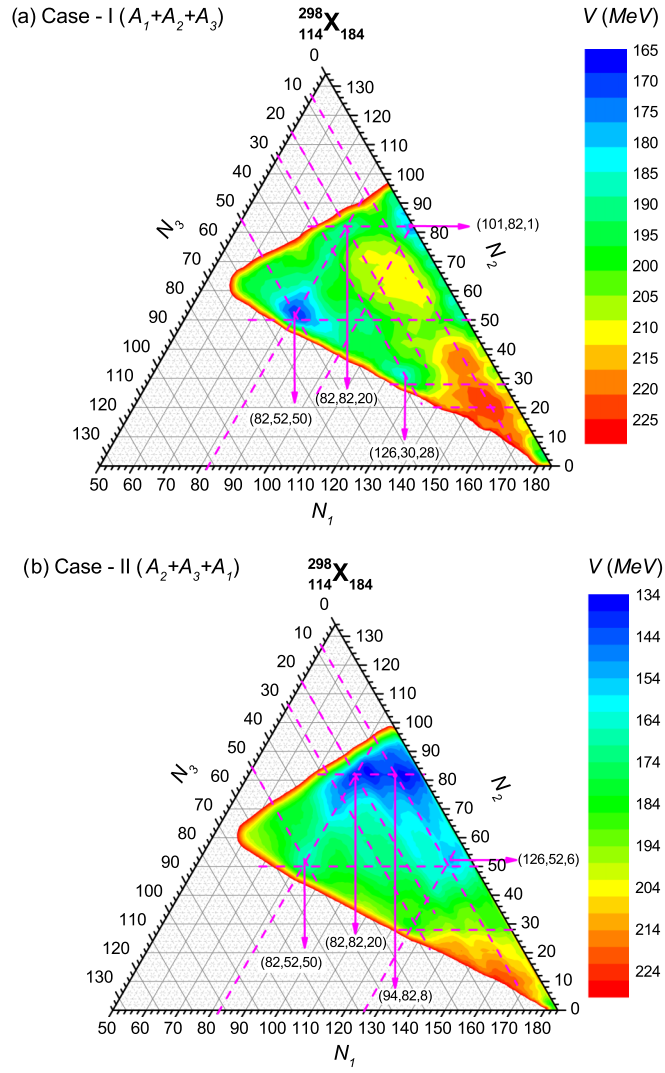

FIG. 6. Potential energy surfaces of neutron-minimized ternary fission fragments at touching configuration for the arrangements (a) Case I (upper) and (b) Case II (lower) in the ternary fission of $^{298}_{114}$X.

groups for a given parent nucleus depends upon the availability of experimental masses we use.

From all the possible groups thus obtained, in each group, we search for a combination having minimum potential energy among all the combinations. This two-dimensional minimization can be done separately for the different arrangements of the fragments, namely Cases I, II, and III.

Figures 4–7 present the ternary plots of the potentials as a function of charge numbers and neutron numbers. The potential energy surfaces of two-dimensional proton-minimized combinations are presented in the ternary plots of Figs. 4(a), 5(a), and 5(b) and neutron-minimized combinations are presented in the ternary plots of Figs. 6(a), 7(a), and 7(b) corresponding to the parent nuclei $^{298}_{114}$X, $^{304}_{120}$X and $^{310}_{126}$X, respectively, for the arrangement of Case I. Figures 4(b) and 6(b) correspond to the arrangement of Case II of the parent nucleus $^{298}_{114}$X for proton and neutron minimization, respectively. In these figures, the magic numbers are shown as dashed lines to see the importance of closed shell effects in the ternary fragmentation. For the three nuclei considered, it is seen that the potential energy is possessing a deeper minimum in the true ternary fission region than in any other region for the arrangement of Case I irrespective of whether the minimization is done with respect to proton or neutron.

In Figs. 4(a) and 6(a), the ternary combination corresponding to the deep minimum is $^{132}_{50}$Sn + $^{84}_{32}$Ge + $^{82}_{32}$Ge, which is present in the true ternary fission region. The next minimum is at the charge numbers $Z_1 = 78$, $Z_2 = 18$, and $Z_3 = 18$ and/or neutron numbers $N_1 = 126$, $N_2 = 30$, and $N_3 = 28$ corresponding to the ternary combination $^{204}_{78}$Pt + $^{48}_{18}$Ar + $^{46}_{18}$Ar. Another notable minimum is corresponding to the combination of $^{162}_{62}$Sm + $^{132}_{50}$Sn + $^{4}_{2}$He in the ternary fission of $^{298}_{114}$X. In Figs. 5(a) and 7(a), the ternary combination corresponding to the deep minimum is $^{134}_{52}$Te + $^{86}_{34}$Se + $^{84}_{34}$Se, which is in the true ternary fission region. In addition to this, there

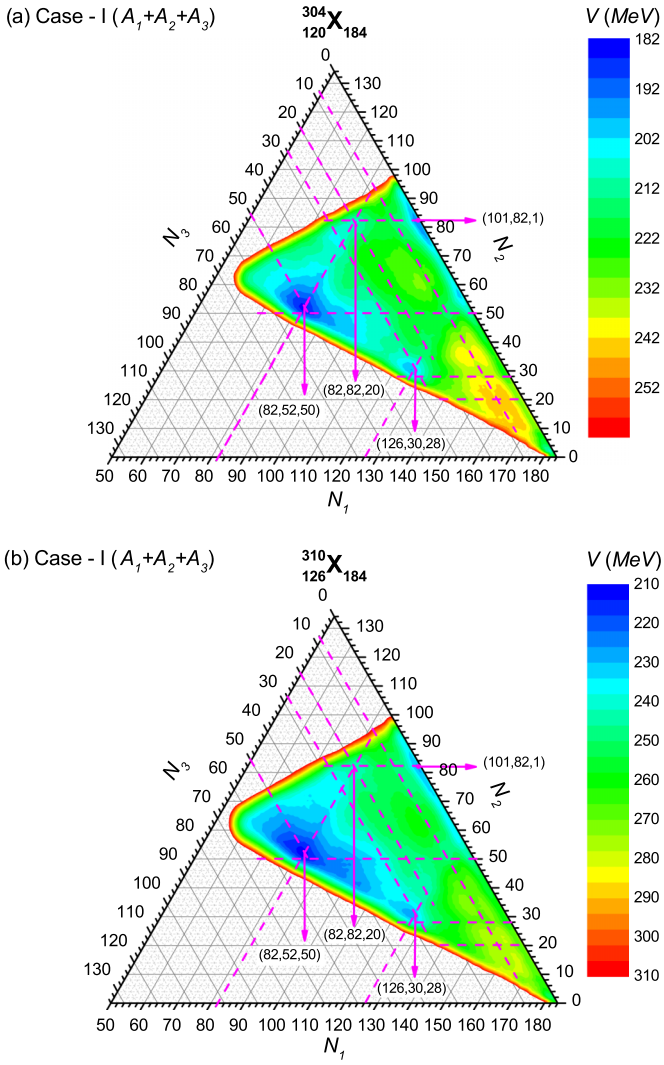

FIG. 7. Potential energy surfaces of neutron-minimized ternary fission fragments at touching configuration for the arrangement Case I in the fission of (a) $^{304}_{120}$X (upper) and (b) $^{310}_{126}$X (lower).

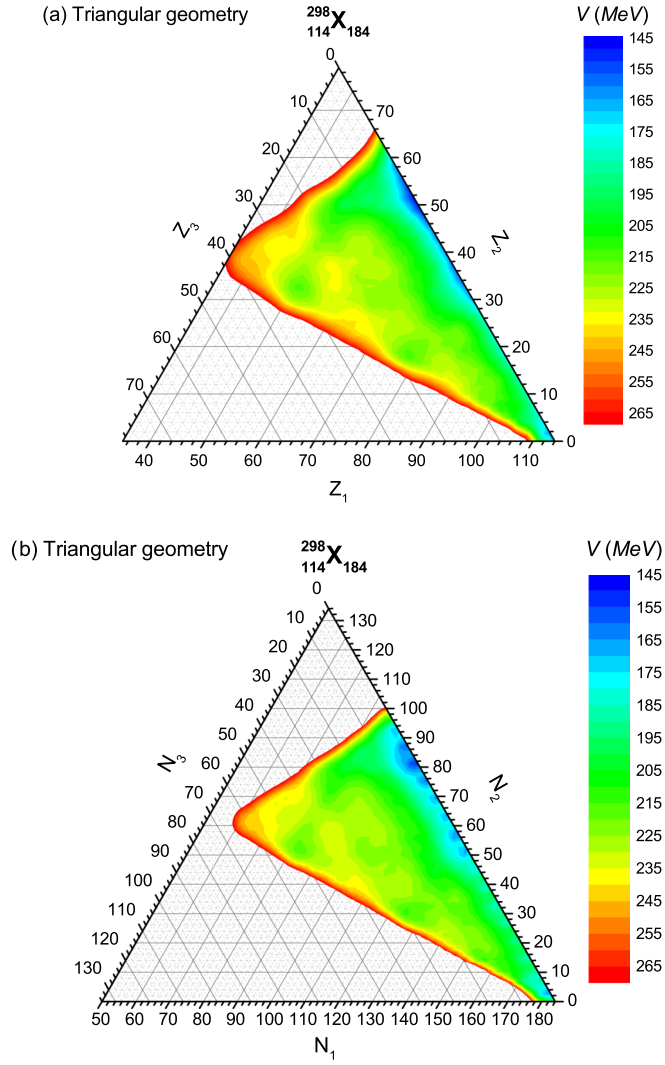

FIG. 8. Potential energy surfaces of ternary fission fragments at touching configuration for the triangular geometry in the fission of $^{298}_{114}$X corresponding to (a) proton minimization and (b) neutron minimization.

is another minimum around the charge numbers $Z_1 = 80$, $Z_2 = 20$, and $Z_3 = 20$ and/or neutron numbers $N_1 = 126$, $N_2 = 30$, and $N_3 = 28$, which corresponds to the ternary combination $^{206}_{80}\mathrm{Hg} + ^{50}_{20}\mathrm{Ca} + ^{48}_{20}\mathrm{Ca}$. In Figs. 5(b) and 7(b), the ternary combination corresponding to the deep minimum is $^{136}_{54}\mathrm{Xe} + ^{88}_{36}\mathrm{Kr} + ^{86}_{36}\mathrm{Kr}$, which is in the true ternary fission region. In addition to this, there is another minimum around the charge numbers $Z_1 = 80$, $Z_2 = 20$, and $Z_3 = 20$, which corresponds to the combination $^{206}_{82}\mathrm{Pb} + ^{52}_{22}\mathrm{Ti} + ^{52}_{22}\mathrm{Ti}$ as seen in Fig. 5(b). Similarly, there is a minimum around the neutron numbers $N_1 = 126$, $N_2 = 30$, and $N_3 = 28$, which corresponds to the ternary combination $^{206}_{82}\mathrm{Pb} + ^{54}_{22}\mathrm{Ti} + ^{50}_{22}\mathrm{Ti}$ as seen in Fig. 7(b).

In addition to these minima, there is a region of minimum along $Z_1 = 50$ (in proton minimization) and $N_1 = 82$ (in neutron minimization) in the ternary fission of all nuclei considered. This suggests that the probability of observing $^{132}_{50}$Sn as one of the fission fragments is higher. In Case II, there is a region of minimum around the charge numbers $Z_1 = 46 - 68$, $Z_2 = 48 - 58$, and $Z_3 = 0 - 20$ [in Fig. 4(b)] and around the neutron numbers $N_1 = 74 - 110$, $N_2 = 74 - 92$, and $N_3 = 1 - 34$ [in Fig. 6(b)] having minimum potential energy. This implies that the possibility of one of the fragments as tin isotope (^{A_1}Sn) is higher in the ternary breakup.

In Refs. [34,35], we have shown that the ternary fission of heavy nuclei has minimum potential energy in the true ternary fission region as well as in a region with $Z_3 = 2$. However, for heavier nuclei such as Cf, the potential energy shows a deep minimum in the region of $Z_3 = 2$ rather than in the true ternary fission region. However, in superheavy nuclei considered for this study, the deep minimum is seen corresponding to the true ternary fission region alone. No other stronger minimum is seen particularly corresponding to the region with $Z_3 = 2$. Although α decay is dominant decay mode for superheavy region, α-accompanied ternary fission seems to be a nonfavorable breakup. The true ternary fission mode is the preferable mode compared to any other modes in

the ternary fission of superheavy nuclei. The results indicate that the possibility of formation of the third fragment (with $Z_3 = 0$–20 or $N_3 = 1$–32) at the center is higher for ternary breakup.

Some of the minima shown in Figs. 4(a), 5(a), and 5(b) do not exactly match with the proton magic numbers. However, the minima marked in Figs. 6(a), 7(a), and 7(b) exactly match with the neutron magic numbers. This result explains the fact that the fragments with neutron magic numbers are the dominant one in the ternary fission of superheavy nuclei. Similarly, fragments with proton magic numbers are dominant ones in the ternary fission of heavy nuclei, as shown in Refs. [34,35].

Figures 8(a) and 8(b) present the potential energy surfaces of $^{298}_{114}$X for the triangular geometry corresponding to proton and neutron minimization respectively. The triangular geometry shows minimum potential energy only for very light third fragments, particularly for $A_3 \leqslant 4$. The deepest minimum corresponds to $Z_1 = 62$, $Z_2 = 50$, $Z_3 = 2$, and $N_1 = 100$, $N_2 = 82$, $N_3 = 2$, a combination involving ^{4}He as the third fragment. The true ternary region, as well as ternary split up with heavy third fragments seen in the calculations of collinear configuration is not present for the triangular configuration. However, for the triangular configuration, the minimum energy seen, at least for some very light particle-accompanied ternary fission events, is lower than the true ternary region present in Case I of collinear configuration but higher than the Case II. This calculation also emphasizes that the triangular geometry is not a favorable configuration for very heavy third-particle-accompanied fission as well as for true ternary fission. Hence, it is suggested that the experimentalists may look for such events in a collinear configuration over triangular configuration.

IV. SUMMARY

The ternary potential energy of all possible ternary combinations of three superheavy nuclei $^{298}_{114}$X, $^{304}_{120}$X, $^{310}_{126}$X are calculated and are minimized by the one-dimensional and two-dimensional minimization procedure. The results of one-dimensional minimization show that there are several prominent three-fragmentation clusters having very low potential energy corresponding to an arrangement in which the lightest fragment is kept at the center. This indicates a stronger probability of formation of the lightest fragment at center for superheavy nuclei. Similar calculations done in Refs. [35,36] for heavy nuclei show no such low potential energy for a range of clusters. Further, the two-dimensional proton and neutron minimization is also carried out. The calculated Q values are found to be high for the true ternary fission region, which is supported by the low potential energy for the true ternary fission region. Obtained results indicate the true ternary mode as a dominant mode to look for in the ternary fission of superheavy nuclei. Further, the prominent combinations are found to associate with magic neutron numbers for superheavy nuclei, which differs for heavy nuclei as reported earlier wherein the proton magic numbers are found to be the dominant ones. Further, true ternary breakup is found to be more favorable than the α-accompanied ternary breakup for superheavy nucleus. Also, it is shown that the triangular configuration is not a favorable configuration to look for heavy third-particle-accompanied fission and true ternary fission.

[1] G. N. Flerov, Synthesis and study of new isotopes and elements, Sov. Atom. Ener. **26**, 160 (1969).

[2] G. N. Flerov, Yu. T.s. Oganessian, A. A. Plev, N. V. Pronin, and Yu. P. Tretyakov, Acceleration of ^{48}Ca ions and new possibilities of synthesizing superheavy elements, Nucl. Phys. A **267**, 359 (1976).

[3] E. O. Fiset and J. R. Nix, Calculation of half-lives for superheavy nuclei, Nucl. Phys. A **193**, 647 (1972).

[4] Yu. Ts, Oganessian, Synthesis of Superheavy Elements, *Proceedings of the International Conference on Nuclear Physics, Munich*, edited by J. de Boer and H. J. Mang (North-Holland/American Elsevier, 1973), Vol. II, p. 352.

[5] R. K. Gupta, A. Săndulescu, and W. Greiner, Synthesis of fermium and transfermium elements using Calcium-48 Beam*, Z. Naturforsch. **32a**, 704 (1977).

[6] M. Bender, K. Rutz, P.-G. Reinhard, J. A. Maruhn, and W. Greiner, Potential energy surfaces of superheavy nuclei, Phys. Rev. C **58**, 2126 (1998).

[7] S. G. Nilsson, C. F. Tsang, A. Sobiczewski, Z. Szymanski, S. Wycech, C. Gustafson, I. Lamm, P. Möller, and B. Nilsson, On the nuclear structure and stability of heavy and superheavy elements, Nucl. Phys. A **131**, 1 (1969).

[8] U. Mosel and W. Greiner, On the stability of superheavy nuclei against fission, Z. Phys. **222**, 261 (1969).

[9] S. Kumar, M. Balasubramaniam, R. K. Gupta, G. Münzenberg, and W. Scheid, The formation and decay of superheavy nuclei produced in ^{48}Ca-induced reactions, J. Phys. G: Nucl. Part. Phys. **29**, 625 (2003).

[10] R. L. Fleischer, P. B. Price, R. M. Walker, and E. L. Hubbard, Ternary fission of heavy compound nuclei in thorite track detectors, Phys. Rev. **143**, 943 (1966).

[11] H. J. Becker, P. Vater, R. Brandt, and A. H. Boos, Ternary fission induced by 540 mev fe ions on uranium, Phys. Lett. B **50**, 445 (1974).

[12] P. Vater and R. Brandt, Ternary fission of uranium induced by 414 MeV Ar-ions as studied with a hole detector, Radiochimica Acta **21**, 191 (1974).

[13] J. F. Wild, P. A. Baisden, R. J. Dougan, E. K. Hulet, R. W. Lougheed, and J. H. Landrum, Light-charged-particle emission in the spontaneous fission of ^{250}Cf, ^{256}Fm and ^{257}Fm, Phys. Rev. C **32**, 488 (1985).

[14] J. Grumann, U. Mosel, B. Fink, and W. Greiner, Investigation of the stability of superheavy nuclei around Z = 114 and Z = 164, Z. Phys. **228**, 371 (1969).

[15] H. Diehl and W. Greiner, Ternary fission in the liquid drop model, Phys. Lett. B **45**, 35 (1973).

[16] H. Diehl and W. Greiner, Theory of ternary fission in the liquid drop model, Nucl. Phys. A **229**, 29 (1974).

[17] H. Schultheis and R. Schultheis, Ternary fission and the stability of superheavy elements, Phys. Lett. B **49**, 423 (1974).

[18] H. Schultheis and R. Schultheis, Possible evidence for superheavy nuclei from spontaneous ternary fission rates, Phys. Lett. B **58**, 384 (1975).

[19] H. Schultheis and R. Schultheis, Prediction of ternary fission rates for element 126, Phys. Rev. C **15**, 1601 (1977).

[20] V. I. Zagrebaev, A. V. Karpov, and W. Greiner, True ternary fission of superheavy nuclei, Phys. Rev. C **81**, 044608 (2010).

[21] S. K. Patra, R. K. Gupta, B. K. Sharma, P. D. Stevenson, and W. Greiner, Exotic clustering in heavy and superheavy nuclei within the relativistic and non-relativistic mean field formalisms, J. Phys. G: Nucl. Part. Phys. **34**, 2073 (2007).

[22] K. Rutz, M. Bender, T. Brvenich, T. Schilling, P.-G. Reinhard, J. A. Maruhn, and W. Greiner, Superheavy nuclei in self-consistent nuclear calculations, Phys. Rev. C **56**, 238 (1997).

[23] M. Bender, K. Rutz, P.-G. Reinhard, J. A. Maruhn, and W. Greiner, Shell structure of superheavy nuclei in self-consistent mean-field models, Phys. Rev. C **60**, 034304 (1999).

[24] R. K. Gupta, S. K. Patra, and W. Greiner, Structure of $^{294,302}120$ nuclei using the relativistic mean-field method, Mod. Phys. Lett. A **12**, 1727 (1997).

[25] S. K. Patra, C.-L. Wu, C. R. Praharaj, and R. K. Gupta, A systematic study of superheavy nuclei for $Z = 114$ and beyond using the relativistic mean field approach, Nucl. Phys. A **651**, 117 (1999).

[26] S. Cwiok, J. Dobaczewski, P.-H. Heenen, P. Magierski, and W. Nazarewicz, Shell structure of the superheavy elements, Nucl. Phys. A **611**, 211 (1996).

[27] K. Manimaran and M. Balasubramaniam, Three-cluster model for the α - accompanied fission of californium nuclei, Phys. Rev. C **79**, 024610 (2009).

[28] K. Manimaran and M. Balasubramaniam, Ternary fission fragmentation of ^{252}Cf for all possible third fragments, Eur. Phys. J. A **45**, 293 (2010).

[29] K. Manimaran and M. Balasubramaniam, Deformation and orientation effects in the ternary fragmentation potential of the ^{4}He- and ^{10}Be-accompanied fission of the ^{252}Cf nucleus, J. Phys. G: Nucl. Part. Phys. **37**, 045104 (2010).

[30] K. Manimaran and M. Balasubramaniam, All possible ternary fragmentations of ^{252}Cf in collinear configuration, Phys. Rev. C **83**, 034609 (2011).

[31] Ternary breakup of $^{298}_{114}$X. K. R. Vijayaraghavan, S. Thakur, R. Kumar, and M. Balasubramaniam, Proc. of DAE-BRNS Symp. on Nucl. Phys. **56**, 548 (2011).

[32] K. R. Vijayaraghavan, W. von Oertzen, and M. Balasubramaniam, Kinetic energies of cluster fragments in ternary fission of ^{252}Cf, Eur. Phys. J. A **48**, 27 (2012).

[33] A. H. Wapstra, G. Audi, and C. Thibault, The AME2003 atomic mass evaluation*: (I). Evaluation of input data, adjustment procedures, Nucl. Phys. A **729**, 129 (2003).

[34] K. R. Vijayaraghavan, M. Balasubramaniam, and W. von Oertzen, True ternary fission, Phys. Rev. C **91**, 044616 (2015).

[35] K. R. Vijayaraghavan, Ph.D. thesis, Bharathiar University, 2015.

[36] K. R. Vijayaraghavan, M. Balasubramaniam, and W. von Oertzen, Collinear versus triangular geometry: A ternary fission study, Phys. Rev. C **90**, 024601 (2014).